ME 530 Homework # 2

Due September 28, 2020

Name_______________

1. Given the Green 's function in class determine and plot the three dimensional displacement distribution for a point force F= (1,1,1).

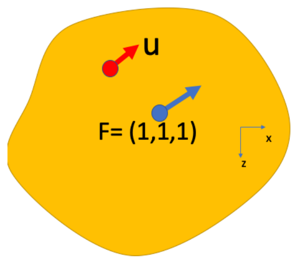

2. In Mura, the Green's function for half space is also given (Equation 15.11, p.95). Considering the Green's function for half space determine the displacement distribution when a point load is applied at the surface in the direction F=(0,0,1). Make a 3D displacement plot in this case.

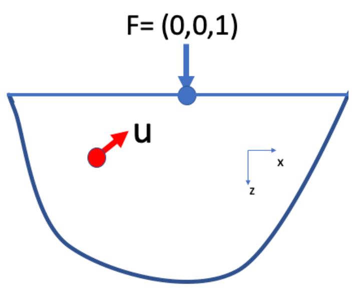

3. In the paper by Tanaka and Mura attached, they give the external field for an inhomogeneity in the Appendix (Equations 42 and 43). Using these equations make a plot of the shear stress field at y=a. Do not derive the equations.

4. We are interested in solving for the spherical inclusion stress field (inside the inclusion) when the eigen strain is (1,0,0). Please determine the constrained strain tensor in this case. Assume poisson's ratio is 0.3. Note that we did the (1,1,1) case in class.

A Theory of Fatigue Crack Initiation at Inclusions

K. TANAKA and T. MURA

The dislocation dipole accumulation model for fatigue crack initiation previously proposed by the authors is extended to an analysis of the fatigue strength reduction due to inclusions in high strength alloys. The initiation of a fatigue crack is determined by an energy criterion under the assumption that the crack initiation takes place when the self strain energy of dislocation dipoles accumulated at the damaged part in the material reaches a critical value. Explicit formulae for the crack initiation criterion in several cases are derived as functions of the applied stress, the inclusion size, the slip band shape, and the shear moduli of the inclusion and matrix. The following three types of fatigue crack initiation at inclusions are considered: the slip-band crack emanating from a debonded inclusion, the inclusion cracking due to impinging of slip bands, and the slip-band crack emanating from an uncracked inclusion. The first mechanism was reported to be operative in high strength steels, while the last two mechanisms were reported in high strength aluminum alloys. The present theoretical results are in good agreement with the experimental data published for each case of fatigue crack initiation at inclusions.

I. INTRODUCTION

THE fatigue strength of high strength alloys is often reduced by the presence of inclusions. Modes of fatigue crack initiation at inclusions depend on the matrix material, types of inclusions, and properties of the interface between inclusions and the matrix. A control of these metallurgical factors is important for alloy designers.

Several microscopic observations have been conducted to clarify several micromechanisms of fatigue crack initiation. In high strength steels, the fatigue limit is much lower than the yield stress, and the fatigue strength is reduced by the presence of inclusions.[1–5] Lankford and Kusenberger[4] summarized a series of stages occurring in fatigue crack initiation at inclusions. The initial stage is the interface debonding of the inclusion from the matrix. Lankford[5] found that this debonding takes place by the first tensile loading even at a stress level close to the fatigue limit. Cracks initiate at the interface with the matrix after this debonding. The major part of the crack initiation life is consumed after the debonding. The initiation of a fatigue crack in the matrix is expected to be caused through an ordinary slip mechanism.[3,4] The influence of the inclusion size on the fatigue limit of high strength steels was analyzed by Morrow.[6] He regarded the inclusions as notches or voids, and utilized the concept of the notch-fatigue strength reduction factor to evaluate the strength reduction due to inclusions. His analytical results agree fairly well with the experimental data reported by Cummings and others.[1,2] His analysis is basically macroscopic, and the microstructural effect on the crack initiation is included in terms of the correction factor by Peterson.[7]

In an aluminum alloy, 2024-T4, on the other hand, Grosskreutz and Shaw[8] observed that the interfacial debonding takes place after a sufficient amount of cyclic slip deformation in the matrix. Morris and his coworkers[9–12] have made extensive observations on crack initiation at inclusions in Al 2219-T851 alloys under maximum cyclic stresses lower than the matrix yielding stress. They found that the inclusions were cracked along the laminated structure or debonded at the inclusion-matrix interface. The inclusion cracking of this type was theoretically analyzed by Chang and others[13] with the use of a dislocation pile-up model at an inclusion. Their analysis was based upon an assumption of dislocation accumulation by cyclic stressing. Chang's analysis was later modified through rather ambiguous approximations to give an agreement with the experimental data on a statistical distribution of inclusion crackings.[11] Another type of fatigue crack initiation at inclusions in 2024-T4 Al alloy was reported by Kung and Fine.[14] They found that a fatigue crack could be initiated along slip bands emanating from an inclusion, and such an inclusion was not necessarily accompanied by debonding. In their experiment, the maximum applied stress was higher than the matrix yielding stress. This type of slip-band cracking will be influenced by the internal stress field due to the inclusion. Any theoretical analysis has not been reported.

Recently, the present authors have proposed a dislocation dipole model for fatigue crack initiation along slip bands in polycrystalline metals.[15] A systematic accumulation of dislocation dipoles under cyclic loading was derived under the assumption of irreversible motion of dislocations. Based on an energy criterion, the analysis yielded a Coffin-Manson type law for crack initiation and a Petch type law for grain size dependency of the fatigue strength.

In this paper, this dislocation dipole model is extended to an investigation on the fatigue strength reduction due to inclusions. For mathematical simplicity, the analysis is carried out for a cylindrical inclusion under anti-plane shear loading.

II. FATIGUE CRACK INITIATION IN HOMOGENEOUS MEDIA

In the present theory of fatigue crack initiation, the forward and reverse plastic flows within slip bands are caused by dislocations with different signs moving on two closely located layers. It is assumed that their movements are irreversible. Based on this model, the monotonic build-up of

K. TANAKA is with the Department of Mechanical Engineering and Mechanics, Lehigh University, Bethlehem, PA 18015. T. MURA is with the Department of Civil Engineering, Northwestern University, Evanston, IL 60201.

Manuscript submitted March 31, 1981.

ISSN 0360-2133/82/0111-0117$00.75/0

dislocation dipoles is systematically derived from the theory of continuously distributed dislocations. The number of stress cycles up to the initiation of a crack about one grain diameter in length is reached when the self strain energy of the accumulated dislocation dipoles reaches a critical value.

Since its fundamental concept is applied here to inhomogeneous media containing inclusions, the theory on fatigue crack initiation in a homogeneous medium[15] is briefly outlined below.

The applied shear stress cycle is shown in Figure 1, where τ_1 is a maximum stress and τ_2 is a minimum stress. The slip deformation is localized within a surface grain in the case of low stress, long-life fatigue of polycrystalline metals such as low carbon steels. The localized slip band extended from $x = -l$ to l is shown in Figure 2a. Points E and F are the grain boundary, where the dislocation motion is blocked. The first forward loading introduces the dislocation pile-up on layer I. The positive back stress (negative with respect to the loading stress) due to dislocations on layer I helps the negative pile-up of dislocations on layer II located very close to layer I during the following reverse loading. The back stress due to dislocations on layer II helps the further dislocation pile-up on layer I during the following loading. Successive reversals of stress, therefore, give the ratcheting accumulation of damage (dislocation dipoles). Although the macroscopic stress-strain hysteresis shows a saturated closed loop, the pile-up of dislocation dipoles increases monotonically by cyclic loading.

The self energy of dislocations introduced in the first loading is

$$U_1 = (\tau_1 - k)^2 \pi l^2 / 2\mu, \qquad [1]$$

where μ is the shear modulus, and k is the frictional stress of dislocations. The increment of the self energy ΔU per half cycle has the same form in each load reversal and is given by substituting $\Delta\tau (= (\tau_1 - \tau_2))$ and $2k$ in places of τ_1 and k in Eq. [1]. Then, we have

$$\Delta U = (\Delta\tau - 2k)^2 \pi l^2 / 2\mu. \qquad [2]$$

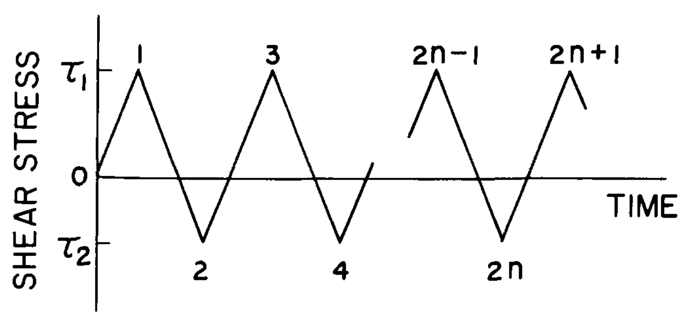

Fig. 1 — Applied shear stress pattern.

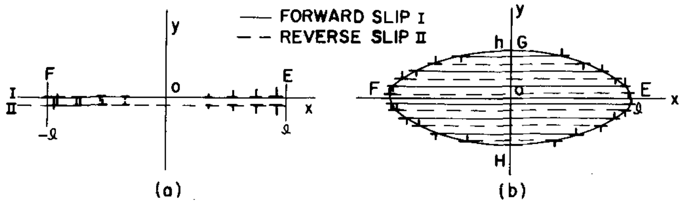

Fig. 2 — Model for dislocation dipole accumulation. (*a*) Isolated slip bands. (*b*) Multiple slip bands.

The total amount of the self energy stored after n cycles is

$$\sum_{i=1}^{2n} U_i = U_1 + 2n\,\Delta U, \qquad [3]$$

where U_i is the increment of the self energy stored in the i^{th} stage of stress reversal. For a long-life fatigue, the first term in the above equation is negligible compared with the second term. The life up to the crack initiation is defined as the number of stress cycles when the following energy condition is satisfied:

$$2n_c \Delta U = 4lW_s, \qquad [4]$$

where W_s is the specific fracture energy for a unit area along the slip band. From Eqs. [2] and [4], we have the following life law:

$$n_c = 4\mu W_s / (\Delta\tau - 2k)^2 \pi l. \qquad [5]$$

Since l is the half grain size, the above equation for $\Delta\tau$ *vs* l is of the Petch type when a crack initiation life is fixed. It is also found that Eq. [5] is equivalent to the Coffin-Manson law when $\Delta\tau$ is expressed in terms of the plastic strain amplitude $\Delta\gamma$.

When the slip band is not isolated but multiple slip bands occur and are constrained in an elliptical grain as shown in Figure 2b, the above formulation must be modified in the following way.

When the range of the applied stress is high, the slip deformation is more uniform and the grain boundary tends to be a preferential site for fatigue crack initiation. This type of crack initiation is treated by use of the inclusion method of Eshelby.[17] The grain is assumed to be an elliptic cylinder embedded in the elastic matrix as shown in Figure 2b, where l and h are semi-major and semi-minor axes, respectively. Under the first forward loading, the uniform plastic strain γ_1 is introduced into the grain. All other grains surrounding this grain are also subject to an average plastic deformation and, therefore, γ_1 is the deviation of plastic strain from the average. This consideration is based on "the self-consistent method." γ_1 is proportional to the average strain. The internal stress τ_1^S caused by γ_1 is calculated from Eq. [40] (in Appendix),

$$\tau_1^S = \mu(2S_{2323} - 1)\gamma_1 = -\mu h \gamma_1 / (h + l), \qquad [6]$$

where the Eshelby tensor S_{2323} is $l/2(h + l)$. The sum of the applied stress τ_1 and τ_1^S should be equal to the friction stress k. Therefore, we have

$$\gamma_1 = (h + l)(\tau_1 - k)/\mu h. \qquad [7]$$

The dislocations introduced by γ_1 are located at the grain boundary as shown in Figure 2b. The strain energy due to these dislocations is (see Appendix)

$$U_1 = -\tau_1^S \gamma_1 \pi h l / 2 = (\tau_1 - k)^2 \pi l (h + l) / 2\mu, \qquad [8]$$

where Eqs. [6] and [7] are used. We can proceed with a similar calculation for opposite dislocation accumulation after a reversed loading. The amount of increase in strain energy due to the new boundary dislocations with the opposite signs, ΔU_G, is given by

$$\Delta U_G = (\Delta\tau - 2k)^2 \pi l (h + l) / 2\mu \qquad [9]$$

which is also valid for each following load reversal. If h approaches zero, Eq. [9] becomes identical to Eq. [2]. For a circular grain, *i.e.*, $h = l$, we have

$$\Delta U_G = (\Delta\tau - 2k)^2 \pi l^2/\mu. \qquad [10]$$

The life up to crack initiation can be derived from the energy criterion as

$$2n_c \Delta U_G = 4\pi l W_G, \qquad [11]$$

where W_G is the specific fracture energy for a unit area of the grain boundary. By substituting Eq. [10] into [11], we have

$$n_c = 2\mu W_G/(\Delta\tau - 2k)^2 l. \qquad [12]$$

This result may be used for crack initiation along the grain boundary in a homogeneous medium. In order to investigate the inclusion effect, the theory must be modified as shown in subsequent sections.

The foregoing analyses are carried out for the case of screw dislocation pile-ups under anti-plane shear loading. In ordinary push-pull or torsional fatigue, the applied stress can be in-plane shear and the dislocations involved for crack initiation are of the edge type. The calculation for those cases is similar and the final equations for the initiation life have the same functional form.[15]

III. FATIGUE CRACK INITIATION AT INCLUSIONS

Classification of Fatigue Crack Initiation at Inclusions

A circular cylindrical inclusion Ω embedded in the matrix is subjected to a uniform anti-plane shear stress, and the matrix and the inclusion are assumed to be isotropic with the shear moduli μ and μ', respectively. The coordinate axes 0x, 0y are taken as shown in Figure 3, and the third coordinate is 0N. The applied stress is perturbed by an inclusion because of the different shear moduli. The stress inside Ω and that immediately outside Ω are easily evaluated by the equivalent inclusion method of Eshelby.[17,19] The stress at an arbitrary external point can also easily be obtained if the stress field outside a corresponding void is known (see Appendix). Under the uniform shear stress τ_1 at infinity, the elastic stresses, τ_{xN} and τ_{yN}, are expressed in the complex form of

$$\tau_{xN} - i\tau_{yN} = -i\tau_1 + i\tau_1 \alpha a^2/z^2, \qquad [13]$$

where $z = x + iy$, a is the inclusion radius, and

$$\alpha = (\mu' - \mu)/(\mu' + \mu). \qquad [14]$$

The stress values of τ_{yN} at points A and B are

$$(\tau_{yN})_A = (1 - \alpha)\tau_1,\ (\tau_{yN})_B = (1 + \alpha)\tau_1. \qquad [15]$$

The stress is maximum at points A and C for $\mu' < \mu$ and at points B and D for $\mu' > \mu$.

As seen in high strength steels, if the strength of the interface between matrix and inclusion is weak enough to break by the first loading without any accompanying plastic deformation, the condition of this debonding is given by the applied interface stress. Since the debonded inclusion behaves like a void, or a notch, the initial crack will start at A or C. The crack will propagate from the interface into the matrix in the very early stage of fatigue, as shown in Figure 3a, and the main part of the fatigue life will be spent in this crack initiation in the matrix. This type of crack initiation is classified here as Type A.

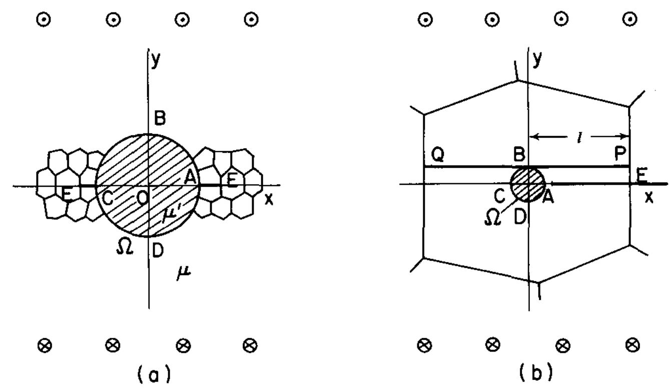

Fig. 3—Types of fatigue crack initiation at inclusions. (*a*) Slip bands emanating from a debonded inclusion (Type A). (*b*) Slip bands emanating from an inclusion (Type C).

If the inclusions and the interface are strong enough not to break in the initial loading, the plastic flow is accumulated in the matrix grain after some time of cyclic loading. The motion of dislocations in the matrix will be blocked by inclusions. The accumulation of dislocations impinging on the inclusion will eventually result in the inclusion debonding or cracking. The inclusion debonding or cracking reported by Morris and his coworkers[9,10] in Al 2219-T851 alloy may be classified under this type. We call this type Type B.

Sometimes, however, these inclusions are not debonded or cracked, but a crack initiates in the matrix from the inclusion interface. This crack initiation is found along a slip band emanating from the point of stress concentration as shown in Figure 3b. This type of fatigue crack initiation was observed by Kung and Fine[14] in Al 2024-T4 alloy. It is named Type C.

Type A Crack Initiation from Inclusions

Fatigue crack initiation from a completely debonded inclusion can be treated like crack initiation from a void or a notch. The stress is maximum at A and C as shown in Figure 3a, and the elastic stress concentration factor is two. The slip bands started from A and C will be blocked at some points E and F which are located at the boundaries of the grains, or at a martensite bundle or packet in high strength steels.[3]

The dislocation dipole accumulation model is applied to AE or FC, where Ω is assumed to be a void. Since the details of the analysis will be published somewhere else,[16] here we discuss only its outline.

The slip bands caused by forward and reverse loadings are stopped at a boundary when the maximum stress τ_1 and the stress range $\Delta\tau$ satisfy the conditions: $\tau_1 > \tau^*$ and $\Delta\tau > 2\tau^*$, where

$$\tau^* = (k/\pi)\,(\pi/2 + \cos^{-1}(a/c))$$
$$c = [(a + l)^2 + a^2]/2(a + l) \qquad [16]$$

and l is the length of the slip bands. Under those conditions, the self energy U_1 due to dislocations caused by the first loading is expressed as

$$U_1 = \tau\gamma_1^T/2 - k\gamma_1^L/2 + \pi a^2 \tau^2{}_1/\mu, \qquad [17]$$

where γ_1^T is the sum of the displacements due to notch and slipbands, and γ_1^L is the displacement caused by slip. They are

$$\gamma_1^T = 2\pi\beta\tau_1(2c^2 - a^2)/\mu + 2ka[3(c^2 - a^2)^{1/2} - 2aI]/\mu + \pi ka^2/\mu$$

$$\gamma_1^L = 4\beta\tau_1[c^2\cos^{-1}a/c - a(c^2 - a^2)^{1/2} + \pi(c^2 - a^2)/2]/\mu + 4ka[(1/\pi + \cos^{-1}a/c)(c^2 - a^2)^{1/2} + 2a \ln a/c - aI]$$

$$\beta = 1 - k/2\pi - k\cos^{-1}(a/c)/\pi\tau_1$$

$$I = \frac{1}{\pi a^2}\int_a^c \frac{t^2}{(t^2 - a^2)^{1/2}} \ln \left|\frac{t(c^2 - a^2)^{1/2} + a(c^2 - a^2)^{1/2}}{t(c^2 - a^2)^{1/2} - a(c^2 - a^2)^{1/2}}\right| dt. \quad [18]$$

The increment of the self energy ΔU in each load reversal is obtained by substituting $\Delta\tau$ and $2k$ for τ_1 and k in Eqs. [17] and [18]. By using this ΔU, we obtain the fatigue crack initiation condition from Eq. [4].

By denoting the stress range required for crack initiation at a given n_c in the inclusion-free material as $\Delta\tau_0$, which is calculated from [5], the reduction of the fatigue strength due to inclusions is obtained as a function of the inclusion size relative to the slip band length. The fatigue strength reduction factor for the inclusion-containing material is defined as

$$K_f = \Delta\tau_0/\Delta\tau. \quad [19]$$

If a cyclic stress range (amplitude) $\Delta\tau$ is given, the reduction of the crack initiation life n_c due to inclusions (relative to the crack initiation life n_{c_0} in the inclusion-free material) is given by

$$n_c/n_{c_0} = \Delta U_0/\Delta U, \quad [20]$$

where ΔU is the energy increment for a half-cycle in the material containing inclusions and ΔU_0 is that the inclusion-free material. ΔU_0 is calculated from [2].

The reduction of the fatigue strength $\Delta\tau/\Delta\tau_0$ (= $1/K_f$) for a constant n_c is plotted in Figure 4 against the inclusion size a relative to the slip band length l, where $\Delta\tau_0/2k$ is taken as a parameter. The fatigue strength $\Delta\tau$ is about equal to $\Delta\tau_0$ for small values of a/l and decreases with increasing inclusion size. For very large inclusions, $\Delta\tau/\Delta\tau_0$ approaches one half, that is, the fatigue strength reduction factor equals the inverse of the elastic stress concentration factor $K_t = 2$.[16] The relation between $\Delta\tau$,$\Delta\tau_0$ and a/l is almost independent of the crack initiation life n_c, which is implicitly a function of $\Delta\tau_0/2k$.

For several values of the applied stress ranges, the reduction of the crack initiation life with a/l is also shown in Figure 4. The amount of reduction is larger for smaller stress ranges. This trend and its inclusion size dependency are in good agreement with the experimental data for SAE 4340 steel reported by Stulen and others.[1] This fatigue strength reduction due to inclusions under a given life is also in accord with the data for the same steel reported by Cummings and others.[2] The higher fatigue strength reduction reported for higher strength materials measured under a constant inclusion size can also be explained by the curves in Figure 4, because higher strength materials have smaller slip band length l.

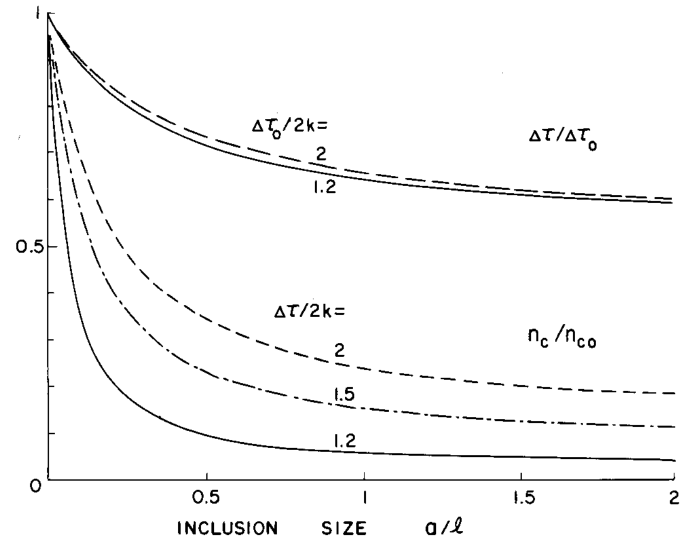

Fig. 4—Reductions of fatigue strength and crack initiation life due to inclusions are plotted against a/l for Type A.

Type B Inclusion Cracking by Impinging Slip Bands

The hard inclusions in Al alloys[8-11,14] will break along the interface before slip band cracking takes place if the inclusion size is not very small. This Type B inclusion cracking is solved by the use of the inclusion method of Eshelby.

Figure 5 illustrates the model of an inclusion Ω within the slip band zone Ω_1. The slip band zone is elliptic with semi-major axis l and semi-minor axis h. The inclusion is assumed to be much smaller than the slip band zone. By neglecting the inclusion at first, the plastic strain γ_1 in Ω_1 is given by Eq. [7]. The stress perturbation due to the elastic inclusion Ω is approximated by the internal stress caused by the eigenstrain $-\gamma_1$ in Ω in an infinite plate.[20] The stress τ_1' inside Ω is calculated as (see Appendix)

$$\tau_1' = \mu\mu'\gamma_1/(\mu' + \mu). \quad [21]$$

The strain energy stored due to the presence of inclusion Ω is

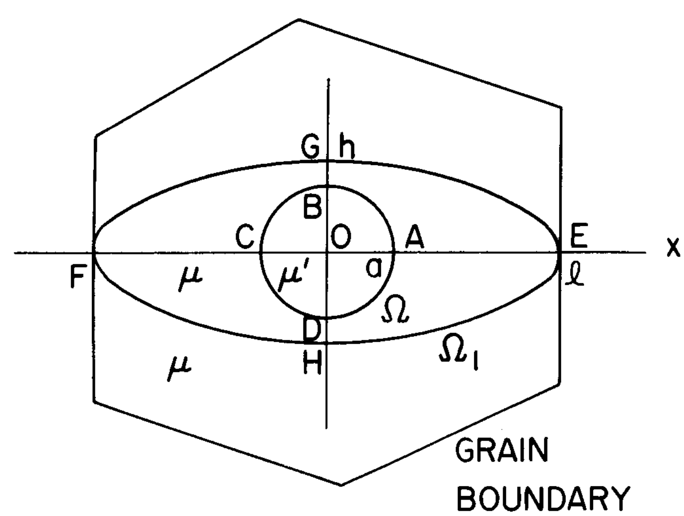

Fig. 5—Inclusion Ω in zone Ω_1 of multiple slip bands (Type B).

$$U_1 = \tau_1' \gamma_1 \pi a^2/2$$
$$= \frac{\mu'}{\mu' + \mu}\left(\frac{h + l}{h}\right)^2 \frac{\pi a^2}{2\mu}(\tau_1 - k)^2, \qquad [22]$$

where Eqs. [7] and [21] are used. The above energy is the strain energy due to Orowan dislocation loops trapped at the inclusion interface as shown in Figure 6a. The interfacial stress is maximum at B and D in Figure 5. This maximum stress is obtained as

$$(\tau_{yN})_B = \mu'(2k + \mu\gamma_1)/(\mu' + \mu)$$
$$= \mu'[\tau_1(h + l)/h - k(l - h)/h]/(\mu' + \mu) \qquad [23]$$

where Eq. [7] is used in the derivation (see Appendix).

Under the assumption that Orowan loops trapped at the inclusion interface are irreversible, the amount of increment of the self strain energy ΔU_I in each load reversal is obtained from Eq. [22], through the usual substitution, as

$$\Delta U_I = \frac{\mu'}{(\mu' + \mu)}\left(\frac{h + l}{h}\right)^2 \frac{\pi a^2}{2\mu}(\Delta\tau - 2k)^2. \qquad [24]$$

The Orowan loops with different signs are accumulated by the cyclic loading as shown in Figure 6b. The total amount of the strain energy accumulated after n cycles is $U_1 + 2n\Delta U_I$. The interfacial stress after n cycles is the same as in the first loading, and its maximum value is given by Eq. [23]. If the interface breaks through a stress criterion, the cracking should occur in the first loading. Since this situation is already treated as Type A in the preceding section, the energy criterion seems to be appropriate. The number of cycles up to a crack initiation n_c is calculated from

$$2n_c\Delta U_I = 4\pi a W_I, \qquad [25]$$

where W_I is the specific fracture energy for a unit interfacial area. The substitution of Eq. [24] into [25] yields

$$n_c = \frac{\mu' + \mu}{\mu'}\left(\frac{h}{h + l}\right)^2 \frac{4\mu W_I}{(\Delta\tau - 2k)^2}\frac{1}{a}. \qquad [26]$$

When the width of the slip band zone h is smaller than l, the above equation becomes

$$n_c = C\, W_I/[(\Delta\tau - 2k)^2\, l^2 a]$$
$$C = 4\mu(\mu' + \mu)h^2/\mu'. \qquad [27]$$

If the plastic zone spreads over the whole circular grain, *i.e.*, h equals l, n_c is

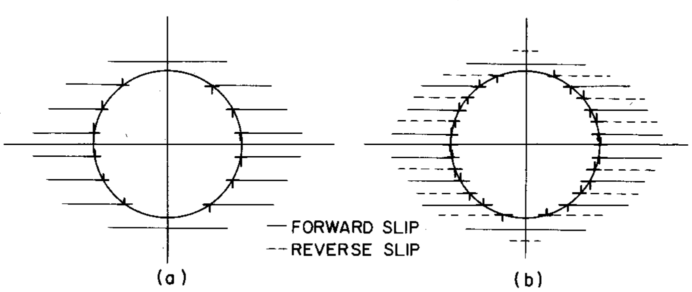

Fig. 6—Model of accumulation of dislocation dipole loops at interface. (*a*) Orowan's dislocation loops. (*b*) Dipole dislocation loops.

$$n_c = (\mu' + \mu)\,\mu\, W_I/[\mu'(\Delta\tau - 2k)^2 a]. \qquad [28]$$

The life law expressed by Eq. [27] is very similar to Chang's formula modified by Morris and James[11] except that the power of l in their equation is one, not two. They proved that his equation agreed with the experiments of inclusion cracking found in fatigue of Al 2219-T851 alloy by taking an appropriate value of coefficient C and also by multiplying with a factor depending on the grain size l.[11] Although Chang did not clarify the coefficient C, the present analysis indicates that it is the function of the shear moduli of matrix and inclusion, and of the width of the slip band.

It can be seen in Eq. [27] that the number of cycles up to the inclusion cracking is inversely proportional to the inclusion size. For materials containing very small inclusions, the fatigue crack starts at slip bands or grain boundaries before inclusions are cracked. Therefore, it can be concluded that the smaller number of cycles between those given by Eqs. [5] to [12] and [27] gives the actual crack initiation life. The small inclusion does not affect the fatigue life as reported by several investigators.[8,14]

Type C Slip Band Crack Emanating from Uncracked Inclusion

The stress is maximum at B and D shown in Figure 3b at the interface of an elastic inclusion harder than the matrix. The fatigue crack initiates at the slip band emanating from B and spreading along PBQ. The stress distribution of τ_{yN} along PBQ is obtained by substituting $z = x + ia$ into Eq. [13] as

$$\tau_{yN} = \tau_1 + \tau_1\alpha a^2(a^2 - x^2)/(a^2 + x^2)^2, \qquad [29]$$

where τ_1 is the applied stress at infinity. If the inclusion is surrounded by a uniform plastic strain γ_1 in the matrix, the misfit stress is superimposed on [29]. Then, the total stress along PBQ becomes (see Appendix)

$$\tau_{yN} = k + [(\mu' - \mu)k + 2\mu'(\tau_1 - k)]a^2(a^2 - x^2)/(a^2 + x^2)^2(\mu + \mu'). \qquad [30]$$

The maximum stress concentration at B is achieved when the inclusion is rigid, *i.e.*, $\mu' = \infty$.

To solve the slip-band crack initiation, the problem of dislocation pile-up along PBQ is to be solved. Since the exact solution has not yet been solved, it will be approximated by the problem of dislocation pile-up under the stress distribution of Eq. [29] or [30] in a homogeneous, infinite plane. The following analysis is carried out for the case of a rigid inclusion where the maximum reduction of the fatigue strength is expected.

First, the slip-band cracking in an elastic matrix will be given. The equilibrium equation of dislocations with density $D_1(x)$ under the initial loading τ_1 is expressed as[21]

$$\tau_1^P(x) + \tau_1^A(x) - k = 0 \qquad [31]$$

where

$$\tau_1^P(x) = (\mu/2\pi)\int_{-l}^{l} D_1(x')dx'/(x - x),\ \tau_1^A(x) = \tau_1 + \tau_1 a^2(a^2 - x^2)/(a^2 + x^2)^2. \qquad [32]$$

The dislocation density $D_1(x)$ is solved under the condition of unbounded density at $x = \pm l$ as[21]

$$D_1(x) = \frac{2}{\pi\mu}\frac{1}{(l^2 - x^2)^{1/2}}\int_{-l}^{l}(l^2 - x'^2)^{1/2}\frac{\tau_1^A(x') - k}{x - x'}dx'$$
$$= \frac{2\beta_0\tau_1}{\mu}\frac{x}{(l^2 - x^2)^{1/2}}$$
$$+ \frac{2\tau_1}{\mu}\frac{a^3x(3a^2 + 2l^2 + x^2)(l^2 - x^2)^{1/2}}{(a^2 + l^2)^{3/2}(a^2 + x^2)^2} \qquad [33]$$

where

$$\beta_0 = 1 - k/\tau_1 + a^3/(a^2 + l^2)^{3/2}. \qquad [34]$$

The dislocations are blocked at P and Q when β_0 is positive, with which the present analysis is concerned. The opening displacement $\phi_1(x)$ caused by the dislocation density $D_1(x)$ is

$$\phi_1(x) = \int_x^l D_1(x')dx'$$
$$= 2\beta_0\tau_1(l^2 - x^2)^{1/2}/\mu + 2\tau_1[a^3/(a^2 + x^2)]$$
$$[(l^2 - x^2)/(l^2 + a^2)]^{3/2}/\mu. \qquad [35]$$

The self strain energy U_1 due to dislocations is derived by using Eqs. [31] and [35] as follows:

$$U_1 = -(1/2)\int_{-l}^{l}\tau_1^P(x)\phi_1(x)dx$$
$$= (\pi/2\mu)(\tau_1 - k)\{\beta_0\tau_1 l^2 + 2\tau_1 a^2[1 - a(3l^2 + 2a^2)$$
$$/2(l^2 + a^2)^{3/2}]\} + (\pi/\mu)\beta_0\tau_1^2 a^2$$
$$\cdot[1 - a/l^2 + a^2)^{1/2}] + (\pi/\mu)\tau^2 a^5$$
$$\cdot[(4a^4 + 2a^2l^2 + l^4)/4a^3(l^2 + a^2)^{1/2} - 1]/(l^2 + a^2)^{3/2}. \qquad [36]$$

The increment of strain energy ΔU is obtained by substituting $\Delta\tau$ and $2k$ for τ_1 and k in the above equation. The energy criterion for fatigue crack initiation along the slip band is given by Eq. [4]. The reduction of fatigue strength at a fixed crack initiation life and the reduction of crack initiation life under a fixed value of applied stress amplitude are calculated similarly as Type A cracking. Figure 7 indicates the variations of $\Delta\tau/\Delta\tau_0$ and n_c/n_{c_0} with the inclusion size a relative to the grain size l. Both the fatigue strength and the crack initiation life are about the same as the inclusion-free material for small inclusion sizes, and tend to decrease with inclusion size. The combined effect of inclusion size and grain size on the fatigue strength agrees with the report by Kung and Fine[14] for Al alloys.

The analysis is easily carried out for the case of a plastic matrix by using the stress distribution of Eq. [30]. The strain energy U_1 introduced by the initial loading τ_1 is

$$U_1 = (\tau/\mu)(\tau_1 - k/2)a^2l^2(2a^2 + l^2)/(a^2 + l^2)^2. \qquad [37]$$

The reduction of the crack initiation life by inclusions is shown in Figure 8 for three cases of the applied stress $\Delta\tau$. When the inclusion size becomes small, the crack initiation life through the present mechanism is longer than that through the slip-band cracking operating in inclusion-free materials. Therefore, the latter mechanism is responsible for actual initiation of a fatigue crack.

IV. CONCLUSIONS

Based on the inclusion strength relative to the matrix, the types of fatigue crack initiation at inclusions in high strength alloys can be classified into three: the slip-band crack emanating from a debonded inclusion, inclusion cracking (or debonding) by impinging slip bands, and the slip-band crack emanating from an uncracked inclusion. The crack initiation of the first type is operative in high strength steels; those of the latter two types are responsible for fatigue in high strength aluminum alloys. A fatigue crack initiation criterion is postulated in which a critical value of the accumulated self strain energy is reached due to dislocation dipole accumulation.

Fatigue crack initiation from a completely cracked inclusion is simulated by slip-band crack initiation from a notch.

The inclusion cracking caused by multiple slip bands impinging upon the inclusion is solved with the use of the inclusion method of Eshelby. The fatigue damage is accumulated in the form of Orowan loops of dislocation dipoles trapped at the interface between an inclusion and a matrix. The fatigue life is determined as the time when the strain

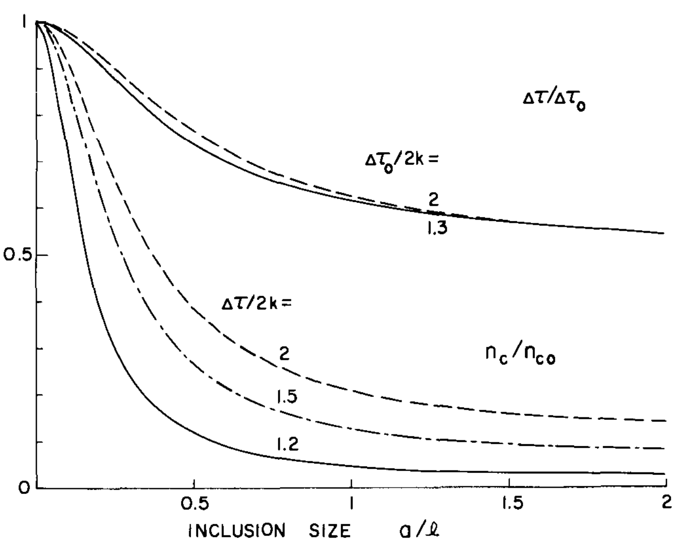

Fig. 7 — Reduction of fatigue strength and crack initiation life by inclusions in an elastic matrix (Type C).

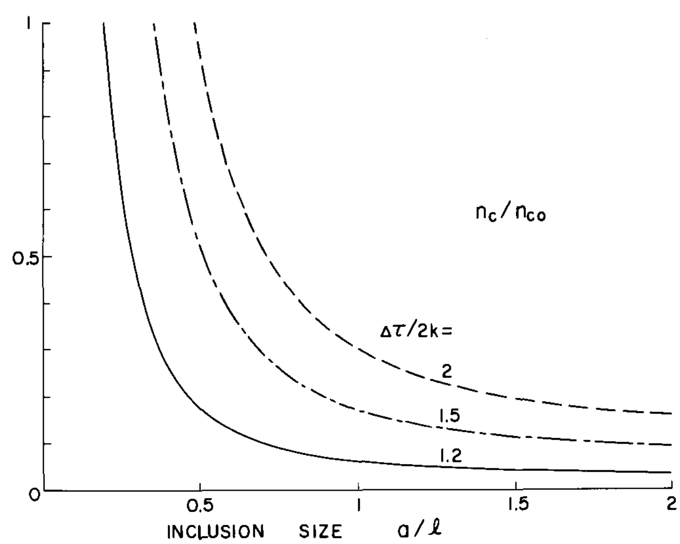

Fig. 8 — Reduction of fatigue crack initiation life by inclusions in a plastic matrix (Type C).

energy of accumulated dislocation dipoles reaches a critical value.

The quantitative relations derived by the present theory explain the reduction of the fatigue strength due to inclusions at a given crack initiation life, and the reduction of the crack initiation life at a given constant range of the applied stress. These reductions depend on the inclusion size and properties of inclusions and matrices. The theoretical results are, at least qualitatively, in good agreement with experimental data reported previously. A quantitative comparison between the theory and the experiments will be conducted in the future.

APPENDIX

Stress Field and Energy of Ellipsoidal Inclusion under Anti-Plane Shear

An isotropic ellipsoidal inclusion Ω with the shear modulus μ' is embedded in an isotropic matrix with the shear modulus μ. Let the inclusion have an eigenstrain $\varepsilon_{yN} = \gamma_P/2$ and the material be subjected to the applied stress $\tau_{yN} = \tau$ at infinity. The stress inside Ω can be solved by the equivalent inclusion method proposed by Eshelby.[17] The eigenstrain ε^*_{yN} for an equivalent inclusion is determined by

$$\begin{aligned}\tau + \tau^I_{yN} &= 2\mu'(\varepsilon^A_{yN} + 2S_{2323}\,\varepsilon^*_{yN} - \gamma_P/2)\\ &= 2\mu[\varepsilon^A_{yN} + (2S_{2323} - 1)\varepsilon^*_{yN}],\end{aligned} \quad [38]$$

where S_{2323} is Eshelby tensor and $\varepsilon^A_{yN} = \tau/2\mu$, and τ^I_{yN} is the perturbation component of the stress inside Ω. From Eq. [38], we have

$$\begin{aligned}\varepsilon^*_{yN} &= -(\mu' - \mu)\varepsilon^A_{yN} - \mu'\gamma_p/2]/[\mu + 2(\mu' - \mu)S_{2323}]\\ \tau^I_{yN} &= (1 - 2S_{2323})[(\mu' - \mu)\tau - \mu'\mu\gamma_p]/\\ &\quad [\mu + 2(\mu' - \mu)S_{2323}].\end{aligned} \quad [39]$$

When τ is absent, ε^*_{yN} and τ^I_{yN} become

$$\begin{aligned}\varepsilon^*_{yN} &= \mu'\gamma_p/2[\mu + 2(\mu' - \mu)S_{2323}]\\ \tau^I_{yN} &= -(1 - 2S_{2323})\mu'\mu\gamma_p/[\mu + 2(\mu' - \mu)S_{2323}].\end{aligned} \quad [40]$$

The strain energy due to eigenstrain γ_p is[18]

$$U = -\tau^I_{yN}\,\gamma_p\Omega/2. \quad [41]$$

When an elastic inclusion is embedded in the plastic matrix with uniform plastic strain γ_1, the stress and the energy can be calculated by substituting $\gamma_p = -\gamma_1$ into the above equations.[20]

Eshelby gave the formulae to evaluate the stress field outside an inclusion. Since his formulae are rather complex, we use an alternate method to evaluate the external field by using the knowledge of the stress field outside a void with identical dimensions. As illustrated in Figure 9, the stress field of a general ellipsoidal inclusion (a) is equal to the sum of two stress fields: the stress field (b) for a void with an identical shape under remote applied stress $-\sigma^I_{ij}$, and the uniform stress field (c) of $\sigma^A_{ij} + \sigma^I_{ij}$, where σ^A_{ij} is the applied stress and $-\sigma^I_{ij}$ is the stress disturbance within Ω. The equivalency of the stress boundary condition is obvious and that of displacement can be proved very easily.

The complex form of the stresses τ^V_{xN} and τ^V_{yN} for a circular cylindrical void under the remote stress $-\tau^I_{yN}$ can be solved with the use of the complex function[16] as

$$\tau^V_{xN} - i\,\tau^V_{yN} = i\,\tau^I_{yN}(1 + a^2/z^2) \quad [42]$$

where $z = x + iy$ and τ^I_{yN} is given by the second of Eq. [39]. By superposing the uniform stress $\tau + \tau^I_{yN}$, we have the total stress:

$$\tau_{xN} - i\tau_{yN} = -i\tau + i[(\mu' - \mu)\tau - \mu'\mu\gamma_p]a^2/(\mu' + \mu)z^2 \quad [43]$$

where $S_{2323} = \frac{1}{4}$ is used.

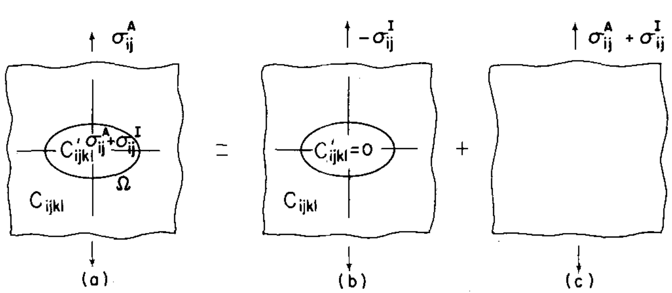

Fig. 9—Stress field of material with inclusion.

ACKNOWLEDGMENTS

This work was supported by the National Science Foundation through the Material Research Center of Northwestern University and by U.S. Army under grant DAAG29-81-K-0090. The authors would like to thank Professor Morris E. Fine for his constructive discussion and suggestions in the present study.

REFERENCES

1. F. B. Stulen, H. N. Cummings, and W. C. Schulte: *Proc. Int. Conf. Fatigue Metals, Inst. Mech. Eng.*, 1956, pp. 439-44.
2. H. N. Cummings, F. B. Stulen, and W. C. Schulte: *ASTM*, 1958, vol. 58, pp. 505-14.
3. S. Taira, K. Tanaka, and K. Watanabe: *Trans. Japan Soci. Mech. Eng.*, 1972, vol. 38, pp. 3067-73.
4. J. Lankford and F. N. Kusenberger: *Metall. Trans.*, 1973, vol. 4, pp. 553-59.
5. J. Lankford: *Int. J. Frac.*, 1976, vol. 12, pp. 155, 56.
6. J. Morrow: unpublished note, Univ. of Illinois.
7. R. E. Peterson: *Notch sensitivity: Metal fatigue*, G. Sin and J. L. Waisman, eds., McGraw-Hill, New York, NY, 1959, pp. 293-306.
8. J. C. Grosskreutz and G. G. Shaw: *Fracture*, P. L. Pratt, ed., Chapman Hall, London, 1969, pp. 620-29.
9. W. L. Morris, O. Buck, and H. L. Marcus: *Metall. Trans. A*, 1976, vol. 7A, pp. 1161-65.
10. W. L. Morris: *Metall. Trans. A*, 1978, vol. 9A, pp. 1345-48.
11. W. L. Morris and M. R. James: *Metall. Trans. A*, 1980, vol. 11A, pp. 850-51.
12. M. R. James and W. L. Morris: unpublished research, Rockwell International, 1980.
13. R. Chang, W. L. Morris, and O. Buck: *Scripta Met.*, 1979, vol. 13, pp. 191-94.
14. Y. C. Kung and M. E. Fine: *Metall. Trans. A*, 1979, vol. 10A, pp. 603-10.
15. K. Tanaka and T. Mura: *J. Appl. Mech., Trans. ASME*, 1981, vol. 48, pp. 97-102.
16. K. Tanaka and T. Mura: *Mechanics of Materials*, in press, (1981).
17. J. D. Eshelby: *Proc. Roy. Soc.*, 1957, vol. A241, pp. 376-96.
18. T. Mura and T. Mori: Applications of micromechanics: Micromechanics, Baifu-kan, Tokyo, 1975, pp. 149-70.
19. J. D. Eshelby: *Proc. Roy. Soc.*, 1959, vol. A252, pp. 561-69.
20. K. Tanaka and T. Mori: *Acta Met.*, 1970, vol. 18, pp. 931-41.
21. A. K. Head and N. Louat: *Australian J. Phys.*, 1955, 8, pp. 1-7.